SYNTHESIS AND LUMINESCENCE OF $SrAl_2O_4$: Eu^{2+}, Dy^{3+}

A. Nor Nazida[1], M. N. Ahmad-Fauzi [1*], M. Nazarov [1,2], A. Azizan [1], and K. Shah Rizal[1]

[1]*School of Materials and Mineral Resources Engineering, Universiti Sains Malaysia, Engineering Campus, 14300 Nibong Tebal, Pulau Pinang, Malaysia*
[2]*Institute of Applied Physics, Academiei Str. 5, Chisinau, MD-2028 Republic of Moldova*
**e-mail: afauzi@eng.usm.my*

(Received 20 March 2011)

Abstract

This study systematically discusses the effects of the synthesis process of $SrAl_2O_4$:Eu^{2+}, Dy^{3+} in reducing the firing temperature and reducing the percentage of concentration of Eu_2O_3 and Dy_2O_3. The influence of firing temperature and rare earth doping on crystal structure, morphology, and its luminescent properties were analyzed by X-ray diffraction (XRD), Raman scattering, Photoluminescence excitation (PLE) and photoluminescence emission (PL) spectroscopy, and scanning electron microscopy (SEM). The emission intensity becomes stronger as the firing temperature increases from 1100°C to 1250°C. $SrAl_2O_4$:Eu^{2+}, Dy^{3+} firing at 1250°C shows the maximum photoluminescence intensity at 0.5 mol % Eu_2O_3 and 1 mol % Dy_2O_3 addition. A phase transformation from $SrAl_4O_7$ to $SrAl_2O_4$ and $Sr_4Al_{14}O_{25}$ is found with increasing firing temperature. The synthesized phosphors reveal the presence of the crystalline monoclinic structure of $SrAl_2O_4$ as a major phase (JCPDS card no. 74-0794) and the intermediate phase orthorhombic structure of $Sr_4Al_{14}O_{25}$. Small amount of doped Eu_2O_3 and Dy_2O_3 has almost no effect on the crystalline phase composition. The proposed firing temperature and mole concentration of the activator and co-activator is lower in comparison with other conventional solid state methods and allows us to obtain the $SrAl_2O_4$:Eu^{2+}, Dy^{3+} phosphor with improved properties.

1. Introduction

Nowadays, long lasting phosphorescence have attracted much attention in a variety of applications, such as lighting source, storage devices, medical instruments, pigments, arts and craft, etc. So far, a big number of different kinds of long persistence phosphor exist now, and most of them have been developed during the past two decades. In recent years, strontium aluminates, especially $SrAl_2O_4$ and $Sr_4Al_{14}O_{25}$ doped with rare earth ions, have been regarded as promising candidates due to their excellent luminescence properties. Several attempts were initially used for synthesis route, such as conventional solid state reaction, sol-gel method, combustion, and microwave heating synthesis. Typically, the synthesis process will be more complex to obtain a good phosphor that consists of high intensity and long persistence glowing properties in an efficient, cheap, and simple way. Solid state reaction process has been extensively used for phosphor synthesis, but this process often results in poor homogeneity leading to high calcination temperature, irregular morphology, and long calcination period [1]. It has been reported that strontium aluminate phosphors were generally prepared at high temperatures (1400–1600°C) for developing a well crystallized structure. Some synthesis and luminescence parameters from recent publications are shown in Table 1.

Table 1. Literature data of synthesis conditions and photoluminescence characteristics of $SrAl_2O_4:Eu^{2+}$, Dy^{3+}

Composition	Structure	Dopant	Temperature	Atmosphere	Spectra		Ref.
			(°C)		PL (nm)	PLE (nm)	
$Sr_4Al_{14}O_{25}$:Eu, Dy	$SrAl_2O_4$ $Sr_4Al_{14}O_{25}$	Eu^{2+} Dy^{3+}	1000- 5h 600- 1300, 5h	Air-prefired Annealing reduction		490	[2]
$SrAl_2O_4$:EuDy, Bx	$SrAl_2O_4$ $Sr_4Al_{14}O_{25}$	Eu^{2+} Dy^{3+}	1000-pre-heat 4h 1200-1300 , 3 h	reduction $10\%H_2+90\%N_2$	320-420	400-520	[3]
$Sr_{1-3}Al_2O_4$: Eu_xDy_y		Eu^{2+} Dy^{3+}	1300- 4h	5 $\%H_2$+95 $\%N_2$	420	520	[4]
	$SrAl_2O_4$ $SrAl_4O_7$	Eu^{2+} Dy^{3+}	1300	Mild reduction Carbon/urea vapor		480-530 640	[5]
$SrAl_2O_4$:EuDy	$SrAl_2O_4$ $Sr_4Al_{14}O_{25}$	Eu^{2+} Dy^{3+}	1300, 4 h	Mild reduction Atmosphere activator carbon		520	[6]
$SrAl_2O_4$:EuDy		Eu^{2+} 1 mol % Dy^{3+} 2 mol %	1250-1300, 6h -4 h	Reduction Atmosphere N_2 + 12% H_2		520	[7]
$SrAl_2O_4$:EuDy	$SrAl_2O_4$: EuDy		1100-1200	Soft-chemical 1-5% H_2 + 95% N_2	260-320	520	[8]

Based on this summary, the selection of firing temperature and atmosphere is important to determine the good photoluminescence spectra and structure as well as microstructure properties. In Table 1, we present a comparison of the properties of $SrAl_2O_4:Eu^{2+}$, Dy^{3+} prepared by different groups of researchers. Most of phosphors were preheated at a suitable temperature of about 1000°C to generate proper precursor powders that enhance the final phase formation. After that, the powders were annealed at a high temperature of 1300°C in a reducing atmosphere (Table 1).

In this study, we focus our attention on the reduction in the firing temperature to improve the luminescent properties by single firing in graphite crucible. A graphite crucible was used to promote the formation of a reducing atmosphere, and this can lower the temperature to save the cost and time. The unique physical and chemical properties of the lanthanide oxides activated by Eu^{2+} ions make them useful in a variety of applications. The emission of these materials is highly efficient, and their emission wavelength heavily depends on host lattice. In the $SrAl_2O_4$ host lattice, the main emission band of Eu^{2+} ions is centered near 520 nm. When another trivalent rare earth ion, such as Dy^{3+} ions, is incorporated into the system, they can enhance the luminescence properties and prolong the afterglow of phosphor. The main goal of this research is to improve the synthesis process, to reduce the firing temperature, and to optimize the concentrations of Eu^{2+} - Dy^{3+}ions in order to obtain the bright persistent phosphors with long-lasting afterglow.

2. Experimental

The conventional solid state reaction is mostly used for the preparation of bulk phosphors. Strontium aluminate phosphors doped with Eu^{2+} and co-doped with Dy^{3+} ($SrAl_2O_4:Eu^{2+}$, Dy^{3+}) were prepared by solid state reaction approach using strontium carbonate ($SrCO_3$; Aldrich, 99.9 %), aluminum oxide (Al_2O_3), europium oxide (Eu_2O_3; Aldrich, 99.99 %), and dysprosium oxide (Dy_2O_3; Aldrich, 99.99 %) as starting materials. A small amount (0.2 mol %) of H_3BO_3 was used as a flux. The raw powders were mixed according to the nominal composition of $SrCO_3$ and Al_2O_3 for the host lattice of $SrAl_2O_4$. To activate this host by Eu^{2+} and Dy^{3+}ions, Eu_2O_3 and Dy_2O_3 were used. The concentration of Eu^{2+} ions and Dy^{3+} ions was optimized separately. An appropriate amount of the starting materials was weighted and mixed. First, the dry milling was used for 30 min, and then a small amount of water was added in the wet-mixing machine for the homogeneity of mixing powders and ground for 30 min. The resulting slurry was dried at 150°C for 3 h to remove the water content. After fully dried, the mixed white powder was placed in a small alumina crucible and then fired consecutively at 1100°C, 1150°C, 1200°C, 1250°C, and 1300°C for 2 h in a mild reducing atmosphere. The physical parameters, such as heating rates of 10°C per minute, cooling rates of 10°C per minute, and a heating time of 2 h, were the same for all samples. The small alumina crucibles with powders were put in a big graphite crucible and then heated at fixed temperature 2 h. The graphite crucible was used to create a reducing atmosphere, to ensure a complete reduction of Eu^{3+} to Eu^{2+}, and to crystallize and form the luminescence centers. The mixing–milling process was used after calcination to obtain a smaller particle size and a homogenous mixture. A set of $SrAl_2O_4:Eu^{2+}$ crystals with different Eu^{2+} ion concentrations of 0.3, 0.5, 0.7, and 1 mol % was synthesized to study the effect of Eu^{2+} activation. Another set of $SrAl_2O_4:Eu^{2+}$, Dy^{3+} crystals with different Dy^{3+} ion concentrations of 1, 2.5, 5, and 10 mol % was also prepared**.**

Structure analysis and phase identification were carried out using XRD and Raman Spectroscopy. A Bruker D8 Advance X-ray Diffractometer with Cu-Kα radiation of wavelength 1.54 Å was applied. Data have been collected by step-scanning 2θ from 10° to 90° and 0.034 s counting time at each step at room temperature. The morphology was observed using a Zeiss Supra 35VP field emission scanning electron microscope. Before SEM observation, the phosphor particles were coated (a thickness of about 5 nm) with Pt-Pd using ion sputter. The photoluminescence excitation and emission spectra were recorded using an IHR 550 UV Fluorescence Spectrometer Horiba Jobin Yvon. All the samples were excited by 325 nm radiation from a pulsed Xenon lamp 450 W. The emission spectra were registered in a wavelengths range of 350 to 625 nm. For measuring the excitation spectra, the monochromator analyzer was set to the maximum wavelength of emission spectra.

Raman measurements were performed at room temperature by Raman Horiba Jobin Vynon HR800UV with excitation through a microscope using the 514.5-nm line of an Ar^+ laser, as well as by a RENISHAW Invia Raman Microscope using an excitation source of 633 nm by the combination of He and Ne sources with an exposure time of 20 s.

3. Results and Discussion

3.1 Effect of firing temperature on $SrAl_2O_4:Eu^{2+}$, Dy^{3+}

Since one of the objectives of this work is to study the effect of firing temperature, samples with the same composition were synthesized at different temperatures and analyzed by XRD. The

study of different firing temperatures is essential in this work. The main reason is to determine the optimum firing temperature which will be used for further phosphor characterization. The Rietveld analysis was performed to determine the structure. Figure 1 shows the XRD patterns of $SrAl_2O_4$:Eu^{2+}, Dy^{3+} annealed at different firing temperatures of 1100 to 1300°C for 2 h in an active carbon atmosphere. It was found that the XRD patterns in a temperature range of 1100 to 1150°C include two phases $SrAl_2O_4$ and $Sr_4Al_{14}O_{25}$, indicating the formation of mixed oxide phases. When the firing temperature was raised to 1200°C, the diffraction peaks of $SrAl_2O_4$, $Sr_4Al_{14}O_{25}$, and $SrAl_4O_7$ appear with the major phase of $SrAl_2O_4$. Moreover, as the firing temperature was increased from 1200 to 1250°C, the XRD peaks were sharper and the stable phases of $SrAl_2O_4$ and $Sr_4Al_{14}O_{25}$ with higher crystallinity could be obtained. The diffraction peak corresponding to $SrAl_4O_7$ disappeared. An increase in peak intensities indicates that the crystallinity also increases as well as the crystal symmetry and size. Two phases $SrAl_2O_4$ and $Sr_4Al_{14}O_{25}$ remain as major and secondary if the firing temperature increases from 1250°C up to 1300°C.

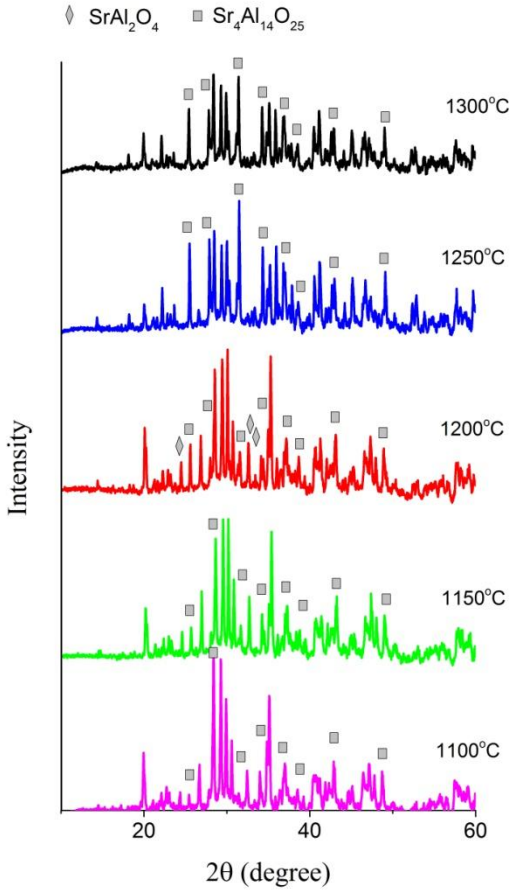

Fig.1. XRD patterns of phosphors at different temperatures.
[◊ = $SrAl_4O_7$, JCPDS - 25-1289; □ = $Sr_4Al_{14}O_{25}$, JCPDS - 52-1876, unmarked peaks belong to $SrAl_2O_4$, JCPDS - 74-0794].

3.2 Effect of Eu^{2+} and Dy^{3+} concentration on crystal structure

X-ray diffraction patterns of $SrAl_2O_4$:Eu^{2+}, Dy^{3+} obtained at 1250°C with different Eu^{2+} concentrations are shown in Fig. 2. The patterns match well with the characteristic diffraction peaks of strontium aluminate phosphor doped with Eu^{2+} and Dy^{3+} [9]. The major formed phase

$SrAl_2O_4$ is monoclinic and corresponds to standard JCPDS card data (74-0794). The secondary observed phase belongs to $Sr_4Al_{14}O_{25}$. This result indicates that the reaction conditions in this work are sufficient to obtain the $SrAl_2O_4$. Small changes of activator concentration do not show any effect on the phase formation.

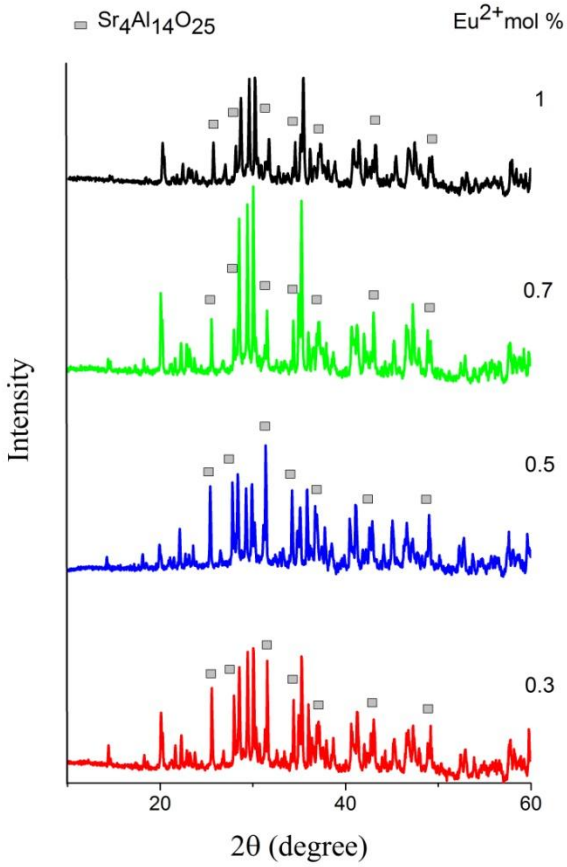

Fig. 2. XRD patterns of phosphors at different Eu^{2+} concentrations.
[□ = $Sr_4Al_{14}O_{25}$ - JCPDS , 52-1876, unmarked peaks belong to $SrAl_2O_4$, JCPDS - 74-0794].

Figure 3 depicts the XRD patterns of $SrAl_2O_4$, $SrAl_2O_4:Eu^{2+}$ and $SrAl_2O_4:Eu^{2+}$, Dy^{3+} firing at 1250°C for 2 h. The XRD patterns show the monoclinic phase diffraction peaks of parent $SrAl_2O_4$ and secondary phase as octahedral $Sr_4Al_{14}O_{25}$. There is no much difference in XRD patterns in the system due to the replacement of Sr^{2+} by Eu^{2+} ions. In addition, a small amount of doped ions of Eu^{2+} and Dy^{3+} has almost no effect on the crystal structure of major phase and secondary phase of octahedral $Sr_4Al_{14}O_{25}$. By addition of Dy^{3+} ions, the intensity of XRD patterns increased indicating an increase in the crystallite size (see Table 2).

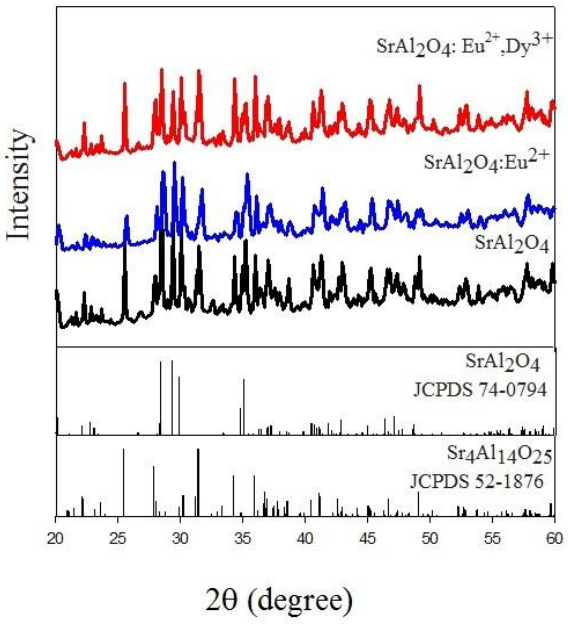

Fig. 3. XRD patterns of $SrAl_2O_4$, $SrAl_2O_4$:Eu^{2+} and $SrAl_2O_4$:Eu^{2+}, Dy^{3+}.

Table 2. Structural parameter of $SrAl_2O_4$, $SrAl_2O_4$:Eu^{2+} and $SrAl_2O_4$:Eu^{2+}, Dy^{3+} for monoclinic $SrAl_2O_4$

	$SrAl_2O_4$	$SrAl_2O_4$:Eu^{2+}	$SrAl_2O_4$:Eu^{2+}, Dy^{3+}
a (Å)	5.1549	5.1569	5.1564
b (Å)	8.8143	8.8217	8.8174
c (Å)	8.4378	8.4440	8.4397
β (°)	93.398	93.398	93.386
V ($Å^3$)	382.711	383.466	383.048
Crystallite size (Å)	913.4	726.6	964.8

Table 2 presents the variation of the lattice parameters and crystallite sizes of $SrAl_2O_4$, $SrAl_2O_4$:Eu^{2+} and $SrAl_2O_4$:Eu^{2+}, Dy^{3+} fired at 1250°C. It is evident from Table 2 that the corresponding lattice parameters (a), (b) and (c), as well as volume unit cells (V), were changed according the Vegard's law because of different activator ionic radius in comparison with the host lattice.

In order to enhance the understanding of the doping effect from the structural point of view, Raman scattering study is a very useful tool in investigating the lattice vibrational modes, which can provide details of lattice vibration changes. The Raman spectroscopy was applied in this work to complement the XRD data, particularly, when it concerns the doping and co-doping of our samples. Two lasers with 514.5 nm and 633 nm wavelengths were used. As the laser wavelength gets shorter, Raman scattering efficiency increases, but, at the same time, the risk of fluorescence also increases. Therefore, we used the 514.5-nm excitation to study only for the undoped host lattice of $SrAl_2O_4$ and 633 nm for the doped materials.

Raman spectrum presented in Fig. 4 was obtained in a spectral range of 100-1000 cm^{-1} using the 514.5-nm excitation wavelength from a continuous wave Ar^+ laser at room temperature. Incident light is focused on a sample through an optical microscope with a spatial resolution of < 2 μm in the backscattering geometry. We repeated these measurements several times from different points of the sample and registered the same spectra as shown in Fig. 4, which confirms the homogeneity of the prepared materials.

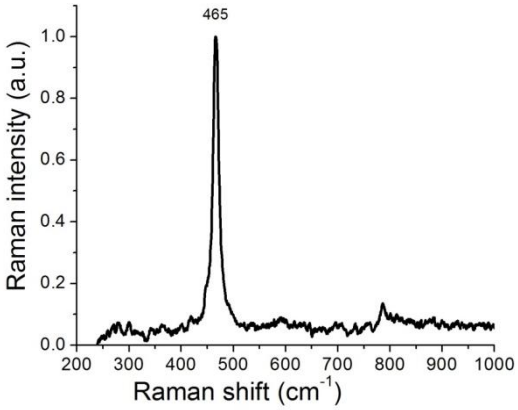

Fig. 4. Raman spectra of the $SrAl_2O_4$ host lattice fired at 1250°C and excited with the514.5 nm laser wavelength.

To a first approximation, we attribute modes at a frequency higher than 600 cm^{-1} to Al–O bond-stretching vibrations and the narrow low-frequency peaks below 250 cm^{-1} (not shown in Fig. 4) to tetrahedral librations or tilts. In the intermediate region, the assignment is impossible; by analogy with other compounds, we assign the most intense band at 465 cm^{-1} to the bending vibration of the O–Al–O angle [10]. This intermediate part of spectra is the most important, and this region (100-600 cm^{-1}) was measured carefully for all samples and shown in Fig. 5.

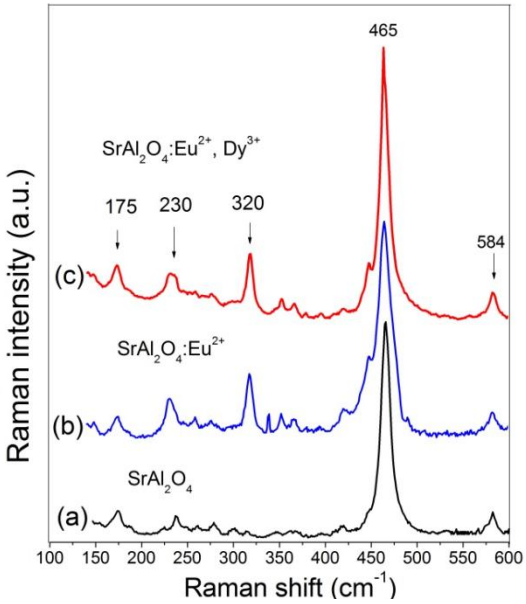

Fig. 5. Raman spectra of $SrAl_2O_4$, $SrAl_2O_4:Eu^{2+}$ and $SrAl_2O_4:Eu^{2+}$, Dy^{3+} fired at 1250°C and excited with the 633-nm laser wavelength.

The profiles (a,b,c) correspond to the Raman spectra of the $SrAl_2O_4$, $SrAl_2O_4:Eu^{2+}$ and $SrAl_2O_4:Eu^{2+}$, Dy^{3+} compositions, respectively. Theoretically, the Raman selection rules allow 81 active modes for monoclinic $SrAl_2O_4$ doped with Eu^{2+} [11]. However, as shown in Fig. 5, in the Raman spectra of Eu^{2+} and Dy^{3+} doped $SrAl_2O_4$, less than 14 active modes were observed, which is partially due to the possible overlap of some symmetry vibrations or the weak features of some Raman bands [12].

All spectra exhibit a ubiquitous 465-cm^{-1} band attributed to the bending of O–Al–O bonds in corner-sharing tetrahedra, indicating that the samples present very closely monoclinic structures.

The Raman spectra of $SrAl_2O_4$:Eu^{2+} and $SrAl_2O_4$:Eu^{2+}, Dy^{3+} are similar to the host $SrAl_2O_4$; however, they show several differences: one small new peak in the main band appears, some peaks especially at 230 and 320 cm^{-1} become stronger, and the width of strongest mode at 465 cm^{-1} has increased for doped phosphors. This result indicates that the lattice of the doped $SrAl_2O_4$ sample is considerably distorted. This is confirmed by the XRD results that show that the crystallite size for this phosphor totally decreases after doping with Eu^{2+}.

3.3 Morphology of $SrAl_2O_4:Eu^{2+},Dy^{3+}$ at different firing temperatures and activator concentrations

SEM study was carried out to investigate the surface morphology and the crystallite size of the synthesized samples. Figure 6 shows SEM images of $SrAl_2O_4:Eu^{2+}$, Dy^{3+} powders obtained at different firing temperatures. Crystal particles formed at lower firing temperature (a) and (b) show a smooth surface and a nonuniform formation of crystallites phosphor. It was observed that the samples fired at 1200°C (c) showed long needle-like crystals on the matrix surface, while the samples fired at 1250°C (d) formed small crystallite phosphor with varying sizes. With a further increase in the firing temperature to 1300°C (e), the surface matrix becomes smooth with solid matrix molten phosphor. Liquid phase sintering occurred at a high temperature because of the addition of flux H_3BO_3. This is believed to be associated with the Eu^{2+} ion content during heat treatment, which accelerates the formation of the crystallite of phosphor. Theoretically, the different shapes and sizes of the phosphor inhibit the absorption of the excitation energy and therefore reduce the emission energy intensity. Phosphor materials must have a narrow size distribution, non-agglomeration, and spherical morphology for good luminescence characteristics [13]. SEM characterization confirms that the optimum synthesis temperature for $SrAl_2O_4:Eu^{2+}$, Dy^{3+} in this study is 1250°C.

The microstructures of heated samples $SrAl_2O_4:Eu^{2+}$, Dy^{3+} with different Eu^{2+} concentrations are shown in Fig. 7. From this observation, we can say that their microstructure was quite different even though the phase form analyzed by XRD was the same. The sample with the lower concentration of activator (a) showed a nonuniform formation of crystallite phosphor. It was observed that the sample with the addition of 0.7 mol% Eu^{2+} (c) showed the homogenous needle-like crystal, while the samples with a high Eu^{2+} concentration of 1 mol % (d) are faceted crystals with varying sizes. This is associated with the Eu^{2+} ion content which accelerates the formation of phosphor crystallite. The multitude of different shapes and sizes of phosphor particles inhibits the absorption of excitation energy and therefore reduces the emission energy intensity.

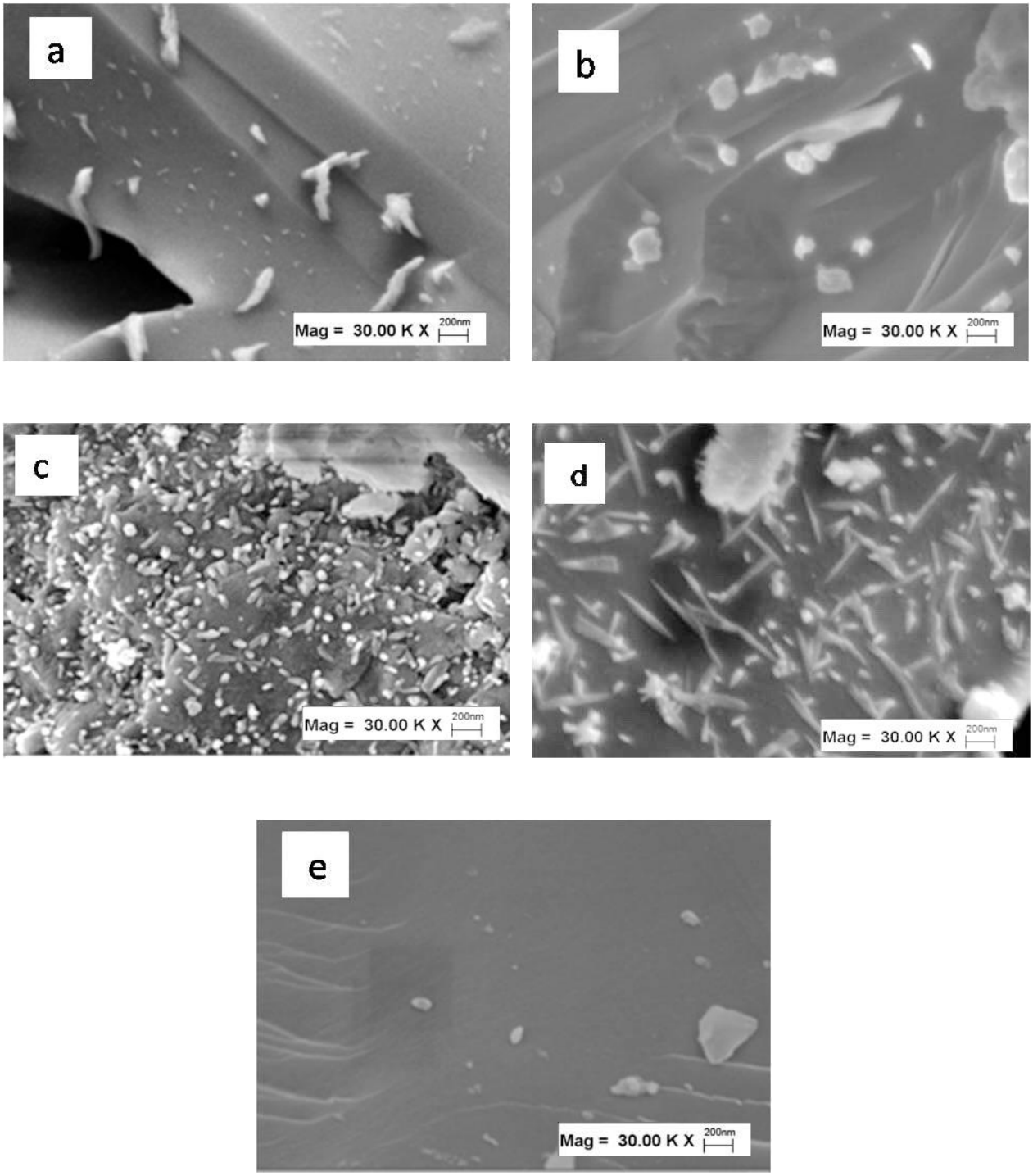

Fig. 6. SEM micrographs of $SrAl_2O_4:Eu^{2+}$, Dy^{3+} phosphor at different temperatures:
a) 1100°C, b) 1150°C, c) 1200°C , d) 1250°C, and e) 1300°C.

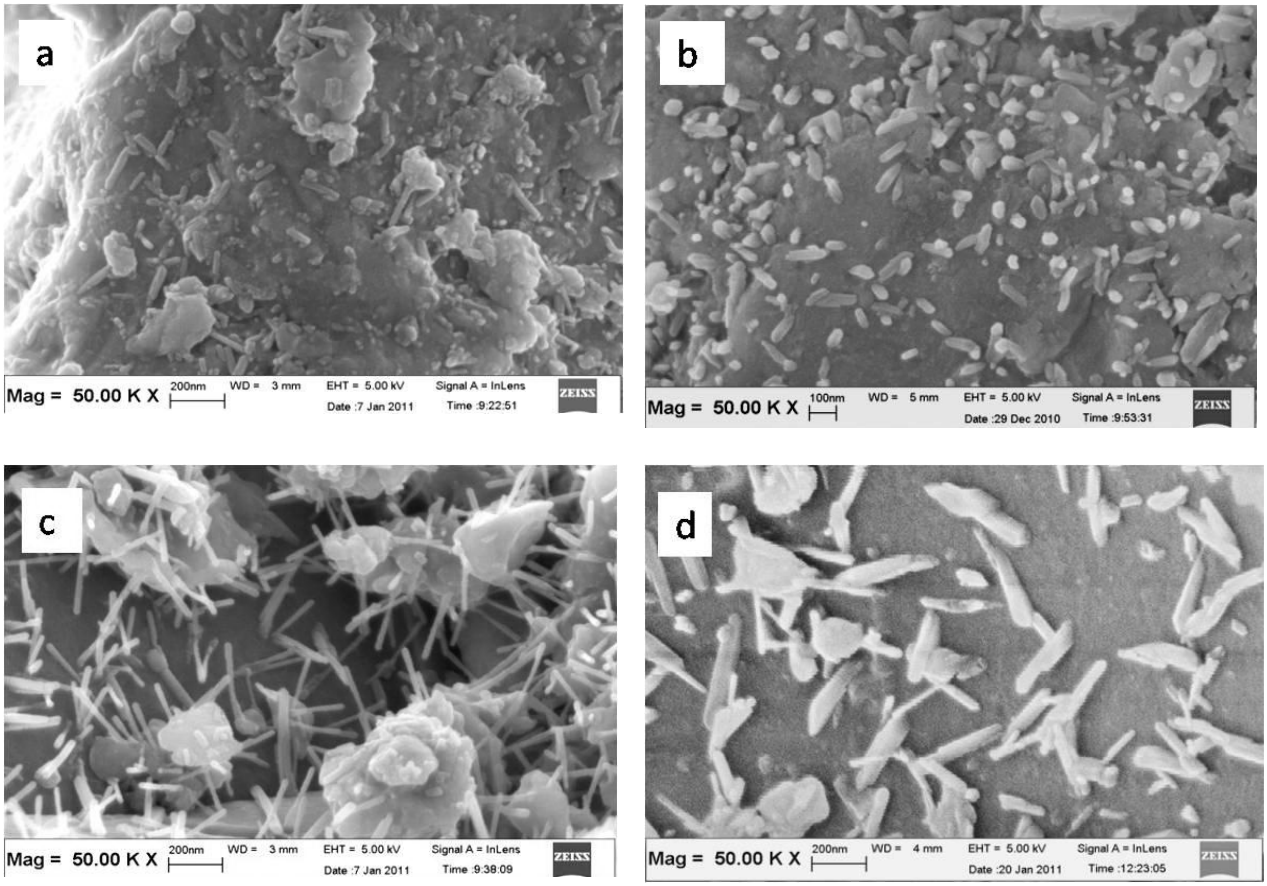

Fig. 7. SEM micrographs of $SrAl_2O_4:Eu^{2+}$, Dy^{3+} phosphor annealed at 1250°C with different Eu^{2+} concentrations: a) 0.3 mol % , b) 0.5 mol %, c) 0.7 mol %, and d) 1 mol %.

Figure 8 shows the morphology of $SrAl_2O_4$, $SrAl_2O_4:Eu^{2+}$ and $SrAl_2O_4:Eu^{2+}$, Dy^{3+} powders prepared at a firing temperature of 1250°C. All the samples show the formation of crystal structures of phosphor. For $SrAl_2O_4$ and $SrAl_2O_4:Eu^{2+}$, the crystal structures are clearer, longer, and inhomogeneous. The shape and size of the crystals are dissimilar. The double activated phosphor $SrAl_2O_4:Eu^{2+}$, Dy^{3+} shows the homogeneity of crystal structure. The shapes are around spherical morphology with homogeneous distribution.

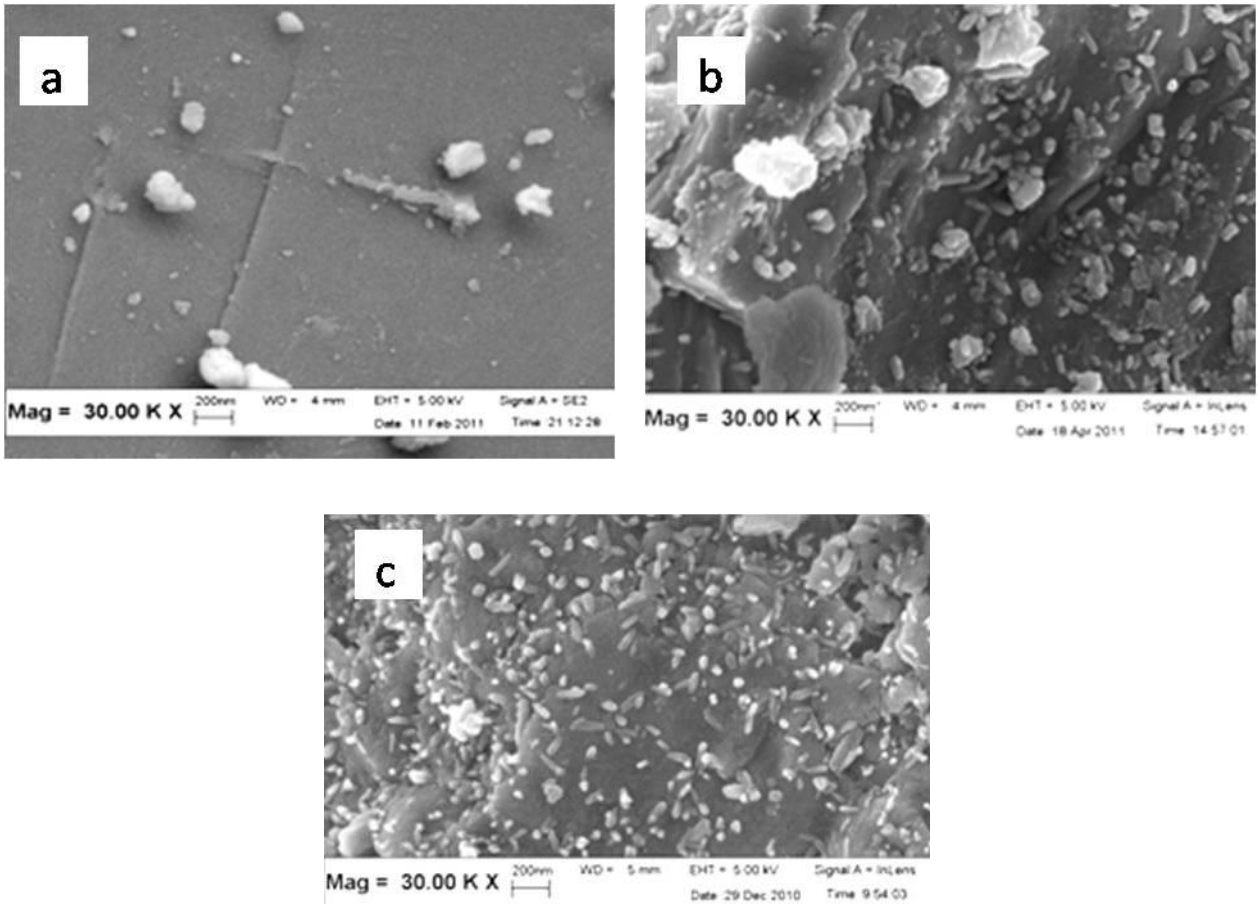

Fig. 8. SEM micrographs of phosphor at a temperature of 1250°C: (a) $SrAl_2O_4$, (b) $SrAl_2O_4:Eu^{2+}$, and (c) $SrAl_2O_4:Eu^{2+}$, Dy^{3+}.

3.4 Effect of activator concentrations and firing temperature on luminescence properties

The main goal in preparing persistent phosphor is the longest and the most intense afterglow emission. Therefore, the process of optimization of the activator concentration is very important. Figures 9 and 10 show the emission spectra of $SrAl_2O_4:Eu^{2+}$ with corresponding Eu^{2+} concentrations of 0.3, 0.5, 0.7, and 1 mol %. For the best sample of $Eu_{0.5}Sr_{0.95}Al_2O_4$ excited with the 325-nm wavelength, the emission band with maximum at 500 nm was registered and it agrees well with the reported spectra profiles in [5-6]. This emission is attributed to the $4f^6 5d^1 \rightarrow 4f^7$ transition in Eu^{2+} ions. No characteristic peaks of Eu^{3+} have been observed in the presented spectra. This means that the active carbon during firing can effectively reduce Eu^{3+} to Eu^{2+}. The Eu^{2+} ions are the luminescence centers for the phosphorescence. A further increase in the Eu^{2+} ion concentration up to 0.7 mol % gradually decreases the emission intensity due to the quenching effect.

There are two main parameters that characterize the persistent phosphors: brightness and long-lasting afterglow.

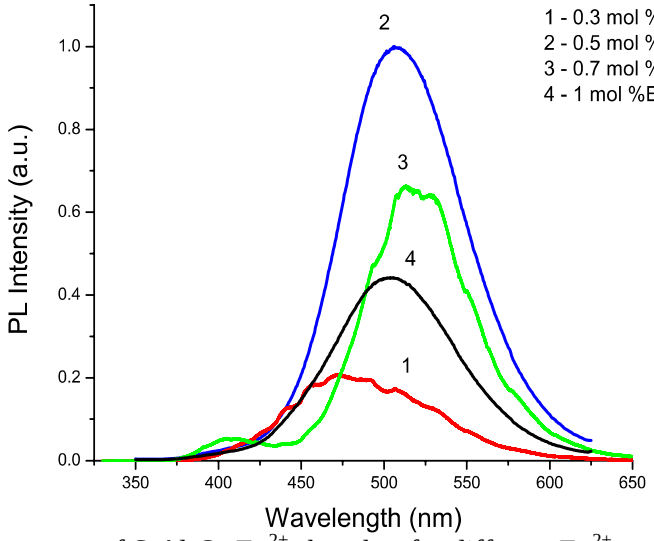

Fig. 9. Emission spectra of $SrAl_2O_4:Eu^{2+}$ phosphor for different Eu^{2+} concentrations.

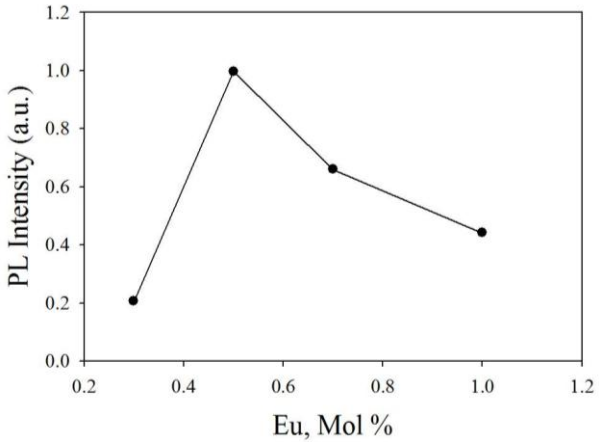

Fig. 10. PL intensity versus Eu concentration in $SrAl_2O_4:Eu^{2+}$.

By co-doping the green-emitting phosphor $SrAl_2O_4:Eu^{2+}$ (already showing a relatively strong and long-lasting afterglow by itself) with the rare earth element dysprosium Dy^{3+}, it is possible to create a material that emits bright light for hours after ending the excitation [14-15].

The luminescence (or phosphorescence for persistent phosphors) intensity of $SrAl_2O_4:Eu^{2+}$, Dy^{3+} doped with various amount of Dy^{3+} ions are presented in Fig. 11. If we increase the Dy^{3+} ion concentration from 0 to 1 mol %, the intensity also increases and attains maximum emission spectra Fig. 11 (2). Then, with a further increase in Dy^{3+} ions, it decreases as shown in Fig. 11. It is obvious that a higher concentration of Dy^{3+} ions in the host lattice will cause the concentration quenching process to decrease the phosphorescence intensity. We can confirm the role of Dy^{3+} ions as hole traps, because there are no emission spectra corresponding to the Dy^{3+} emission in all samples. Dy^{3+} ions also function as energy transporting media and induce the formation of hole traps associated with Sr^{2+} vacancies introduced because of charge compensation [16]. These trap centers generated during the phosphor excitation prolong the glowing times. The phosphorescence intensity depends on the density of traps located at suitable depths. It can be assumed from our experiments that a small amount of Dy^{3+} ions is sufficient to form trap defects in this matrix.

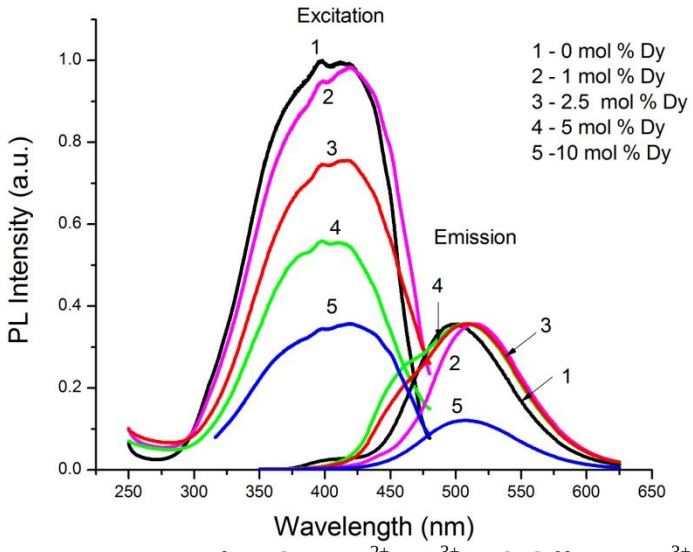

Fig. 11. Excitation and emission spectra of $SrAl_2O_4:Eu^{2+}$, Dy^{3+} with different Dy^{3+} concentrations.

To compare the experimental results, PLE and PL spectra for $SrAl_2O_4:Eu^{2+}$ (1) and $SrAl_2O_4:Eu^{2+}$, Dy^{3+} (2) are shown together in Fig. 12. The emission band peak for only Eu^{2+} doped sample is placed at 500 nm. The codoping of this sample with an optimized Dy^{3+} concentration shifts this peak to 508 nm. This shifting of emission peak is attributed to changes in the crystal field strength around Eu^{2+} ions, when Dy^{3+} ions are introduced. This observation is in good agreement with XRD data, which show that the crystallite size increased for $SrAl_2O_4:Eu^{2+}$, Dy^{3+} resulting in an increase in the crystal symmetry and thus enhancement of the crystal field strength. Two weak resolved bands in the excitation spectra at 398 nm and 419 nm were observed in both PLE spectra (1 and 2). These bands correspond to the crystal field splitting of the Eu^{2+} d-orbitals. We noted here that all the samples were synthesized at 1250°C in a reducing atmosphere in a graphite crucible that totally converted Eu^{3+} to the Eu^{2+} oxidation state. The emission spectra do not show any bands corresponding to Eu^{3+} or Dy^{3+} emissions in all the samples in a range of 350–650 nm. This also confirms that Dy^{3+} ions in the host lattice serve as hole or electron traps and energy transporting media.

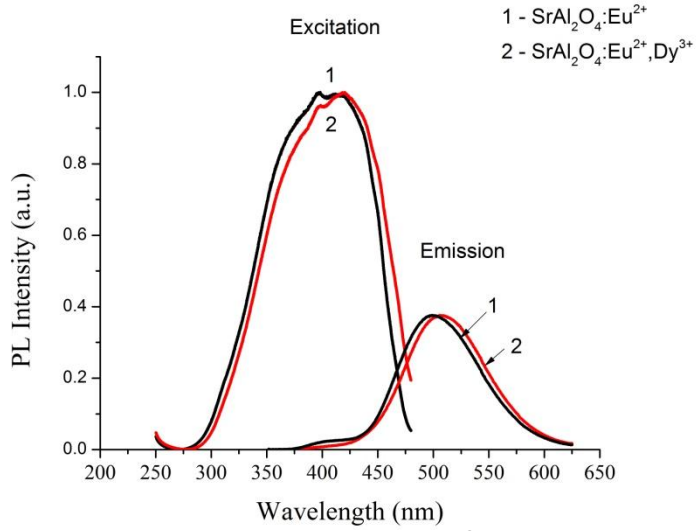

Fig. 12. Excitation and emission spectra for $SrAl_2O_4:Eu^{2+}$ (*1*) and $SrAl_2O_4:Eu^{2+}$, Dy^{3+} (*2*).

The firing temperature is another important parameter that affects the grain size and photoluminescence emission of phosphor. In order to study the role of firing temperature, we synthesized optimized $SrAl_2O_4$:Eu^{2+}, Dy^{3+} (0.5 mol % of Eu^{2+} and 1 mol % of Dy^{3+}) phosphor in the firing range (1100–1300°C). Figure 13 shows the effects of the firing temperature on PL spectra. The shape of spectra and PL intensity significantly changed with temperature variation. The emission spectra of $SrAl_2O_4$:Eu^{2+}, Dy^{3+} increase and shift when the temperature increases from 1100°C to 1250°C. However, their emission intensity is reduced, and the differences between all the samples fired at different temperatures indicate the different natures of Eu^{2+} surrounding [9]. Maximum luminescence was observed at 1250°C. This could probably be attributed to its better crystallinity. For samples fired at 1250°C, it was observed that the sharp emission spectrum peaked at 508 nm under the 325-nm excitation leads to the green luminescence. Poort et al. suggested that the 450 and 520 nm emission bands originate to the $4f^6 5d^1 \rightarrow 4f^7$ transition of Eu^{2+} ions located at the two different crystallographic strontium sites in $SrAl_2O_4$ [2, 17-18]. Two types of Sr^{2+} site are also present in our phosphors; one is surrounded by AlO_4 tetrahedra and the other by AlO_6 octahedra. The ionic radius of Sr^{2+} ($r_{Sr^{2+}}$ = 1.20Å) is quite similar to the ionic radius of Eu^{2+} ($r_{Eu^{2+}}$ = 1.01Å). Hence, the Eu^{2+} ions can easily substitute the Sr^{2+} ion site in the matrix phosphor [8]. However, for samples fired at 1150 and 1200°C, the emission spectra are at 491 nm. It is confirmed that the Eu^{2+} emission efficiency is very sensitive to firing temperature. At a lower temperature of 1100°C, the decrease in the emission intensity may be due to the small amount of Eu^{2+} ions diffused into the host lattice of $SrAl_2O_4$. At a high temperature of 1300°C, the emission intensity was totally reduced, and this is because of the rapid diffusion of Eu^{2+}, Dy^{3+} ions in the host lattice-grain boundary diffusion. The peak positions in the emission spectra depend on the nature of the Eu^{2+} surrounding; therefore, Eu^{2+} ions can emit different visible light in the various crystal fields. Figure 13 suggests that T = 1250°C is an optimum temperature for the best PL emission intensity.

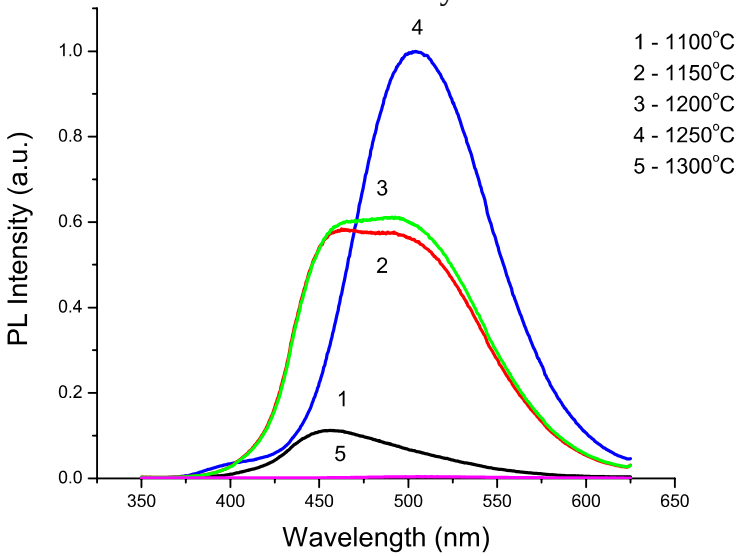

Fig. 13. Emission spectra of the phosphor samples at different firing temperatures.

In Figs. 14 and 15, we show the excitation and emission spectra for $SrAl_2O_4$:Eu^{2+} registered at room and low temperatures.

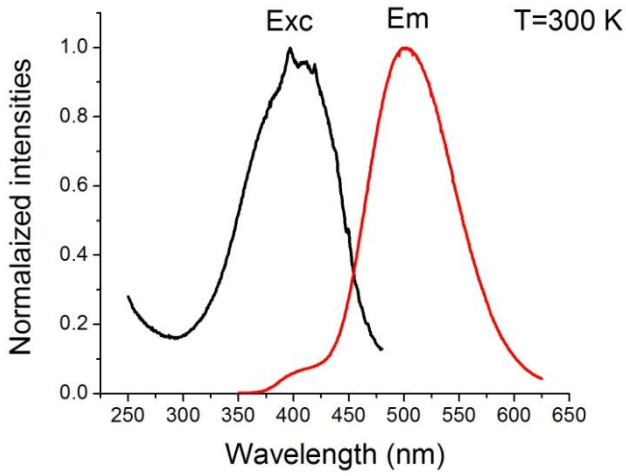

Fig. 14. Normalized excitation (λ_{em}=500 nm) and emission (λ_{exc}= 325 nm) spectra for $SrAl_2O_4:Eu^{2+}$ at room temperature.

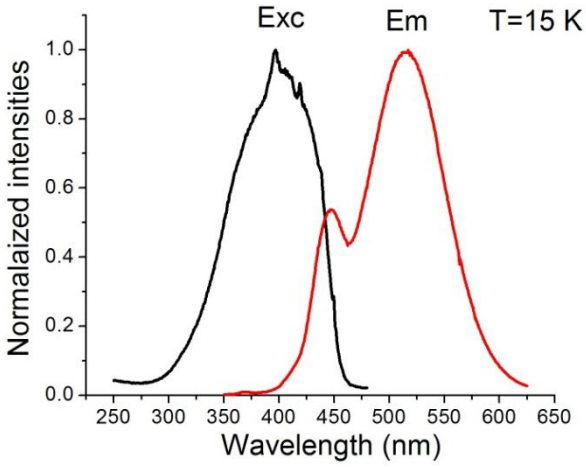

Fig. 15. Normalized excitation (λ_{em}=500 nm) and emission (λ_{exc}= 325 nm) spectra for $SrAl_2O_4:Eu^{2+}$ at 15 K.

One additional band around 450 nm in the emission spectrum was registered at a low temperature. The luminescence at 500 nm is commonly attributed to the parity-allowed electric dipole transition, $4f^6 5d^1 \rightarrow 4f^7$, of the Eu^{2+} ion [19]. The origin of the 450-nm emission is under discussion. Poort et al. suggested that the 450 and 520 nm emission bands originate from the emission of the Eu^{2+} ion located at the two different crystallographic strontium sites [20]. Clabau et al. criticized this assignment and proposed that the 450 nm band arises from the charge transfer from oxygen to residual Eu^{3+} ion that takes place upon UV irradiation and is associated with a hole trapping at Sr^{2+} vacancies [19]. Holsa et al. consider this band as anomalous low-temperature luminescence and suggest that Eu^{2+} ion may exhibit this kind of unusual luminescence from a higher Eu^{2+} 5d state [21]. This band needs a further more detailed examination.

4. Conclusions

Green phosphor $SrAl_2O_4:Eu^{2+}$, Dy^{3+} with improved properties was successfully synthesized by solid state reaction. The optimum firing temperature was greatly reduced to 1250°C. The results revealed the presence of a monoclinic structure of $SrAl_2O_4$ as a major phase and the intermediate phase identified as an orthorhombic structure of $Sr_4Al_{14}O_{25}$. It was found that the combination of 0.5 mol % Eu_2O_3 and 1 mol % Dy_2O_3 is the best for high photoluminescence effect in this system. A new luminescent band at a low temperature around 450 nm in the emission spectrum was observed and discussed.

Acknowledgements

This work was financially supported by Short Term Grant, Universiti Sains Malaysia, under grant No. 304/PBAHAN/60311036 and Post-Graduate Grant Research, 1001/PBAHAN/8044033 to conduct this research.

References

[1] C.H. Lu, and P.C. Wu, J. Alloys and Comp. 466, 457 (2008).
[2] T. Aitasalo, J. Holsa, H. Jungner, J.-C. Krupa, M. Lastusaari, J. Legendziewicz, and J. Niittykoski, Radiat. Meas. 38, 727 (2004).
[3] A. Nag, and T.R.N. Kutty, J. Alloys. Compd. 354, 221 (2003).
[4] X. Lu, W. Shu, Q. Yu, Q. Fang, and X. Xiong, Glass Phys. Chem. 33, 62 (2007).
[5] D. Haranath, V. Shanker, H. Chander, and P. Sharma, J. Phys. D Appl. Phys. 36, 2244 (2003).
[6] S.D. Han, K.C. Singh, T.Y. Cho, H.S. Lee, D. Jakhar, J.P. Hulme, C.H. Han, J.D. Kim, I.S. Chun, and J. Gwak, J.Lumin. 128, 301 (2008).
[7] T. Aitasalo, P. Dere, J. Holsa, H. Jungner, J.C. Krupa, M. Lastusaari, J. Legendziewicz, J. Niittykoski, and W. Strk, J Solid State. Chem. 171, 114 (2003).
[8] Y. Lin, Z. Zhang, F. Zhang, Z. Tang, and Q. Chen, Mater. Chem. Phys. 65, 103 (2000).
[9] R. Melendrez, O. Arellano-Tanori, M. Pedroza-Montero, W.M. Yen, and M. Barboza-Flores, J. Lumin. 129, 679 (2009).
[10] P. Escribano, M. Marchal, M. Luisa Sanjuán, P. Alonso-Gutiérrez, B. Julián, and E. Cordoncillo, J. Solid State Chem. 178, 1978 (2005).
[11] M.A. Salim, R. Hussin, M.S. Abdullah, S. Abdullah, N.S. Alias, S.A.A. Fuzi, M.N.M. Yusuf, K.M. Mahbor, Aip Conf. Proc. 17, 59 (2009).
[12] K.Liang, Y.Qi, C. Lu, J. Raman Spectrosc. 40, 2088 (2009).
[13] X. Yu, C. Zhou, X. He, Z. Peng, and S.P. Yang, Mater. Lett. 58, 2927 (2004).
[14] Abbruscato, V., J. Electrochem. Soc., 118, 930 (1971)
[15] Takasaki H., Tanabe S., and Hanada T., J. Ceram. Soc. Jpn., 104, 322 (1996).
[16] Y. Lin, Z. Tang, and Z. Zhang, Mater. Lett. 51, 14 (2001).
[17] T. Aitasalo, J. Holsa., H. Jungner, M. Lastusaari, and J. Niittykoski, J. Lumin. 94, 59 (2001).
[18] Y. Li, Y. Fang, N. Hirosaki, R.J. Xie, L. Liu, T. Takeda, and X. Li, J. Mater. 3, 1692 (2010).
[19] F. Clabau, X. Rocquefelte, S. Jobic, P. Deniard, M.H. Whangbo, A. Garcia, and T. Le Mercier, Chem. Mater. 17, 3904 (2005).
[20] S. Poort, W.Blokpoel, and G. Blasse, Chem.Mater. 7, 1547 (1995)
[21] J. Holsa, H. Jungner, M. Lastusaari, and J. Niittykoski, J. Alloys. Compd. 323, 326 (2001).